Provided for non-commercial research and education use.
Not for reproduction, distribution or commercial use.

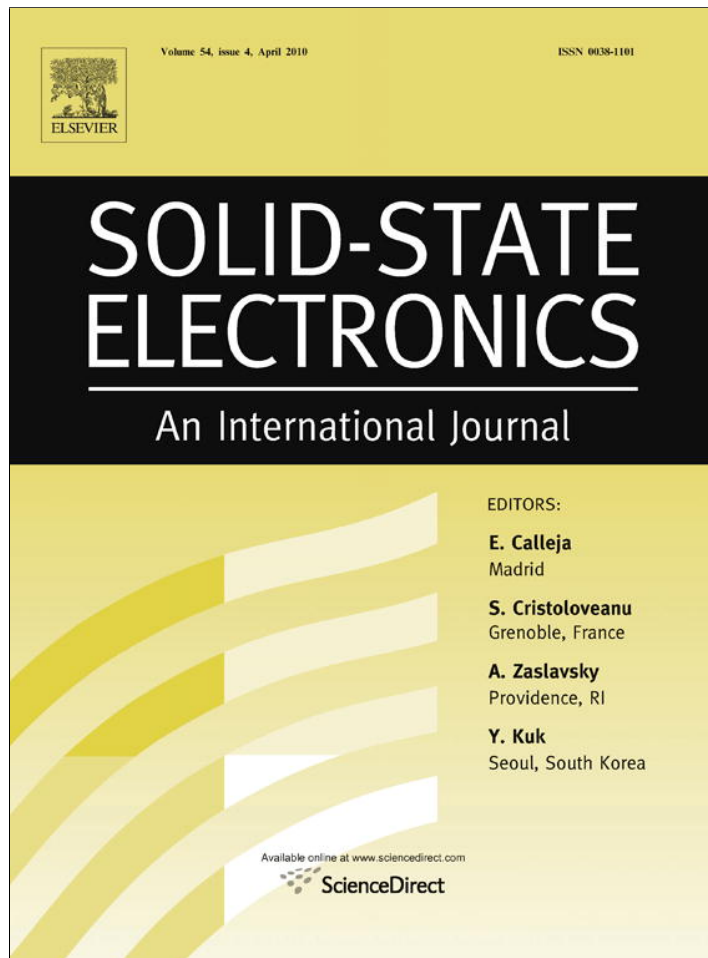

This article appeared in a journal published by Elsevier. The attached copy is furnished to the author for internal non-commercial research and education use, including for instruction at the authors institution and sharing with colleagues.

Other uses, including reproduction and distribution, or selling or licensing copies, or posting to personal, institutional or third party websites are prohibited.

In most cases authors are permitted to post their version of the article (e.g. in Word or Tex form) to their personal website or institutional repository. Authors requiring further information regarding Elsevier's archiving and manuscript policies are encouraged to visit:

http://www.elsevier.com/copyright

Author's personal copy

Solid-State Electronics 54 (2010) 479–483

Contents lists available at ScienceDirect

Solid-State Electronics

journal homepage: www.elsevier.com/locate/sse

Enhancement of electrical performance in In_2O_3 thin-film transistors by improving the densification and surface morphology of channel layers

Hai Zhong Zhang [a], Hong Tao Cao [a,*], Ai Hua Chen [a], Ling Yan Liang [a], Zhi Min Liu [a], Qing Wan [a,b,*]

[a] Division of Functional Materials and Nano Devices, Ningbo Institute of Material Technology and Engineering, The Chinese Academy of Sciences, Ningbo 315201, People's Republic of China

[b] Key Laboratory for Micro-Nano Optoelectronic Devices of Ministry of Education, and State Key Laboratory of Chemo/Biosensing and Chemometrics, Hunan University, Changsha 410082, People's Republic of China

ARTICLE INFO

Article history:
Received 22 July 2009
Received in revised form 10 October 2009
Accepted 6 December 2009
Available online 6 January 2010

The review of this paper was arranged by Dr. Y. Kuk

Keywords:
Indium oxide
Thin-film transistor
RF sputtering
Deposition pressure

ABSTRACT

We report on the fabrication of bottom-gate thin-film transistors (TFTs) using indium-oxide (In_2O_3) thin films as active channel layers. The films were deposited on thermally grown silicon dioxide (SiO_2)/n-type silicon (Si) at room temperature (RT) by radio-frequency (RF) magnetron sputtering. The effect of deposition pressure on the performance of In_2O_3-TFTs was investigated in detail. A significant improvement of the device performance was observed for In_2O_3-TFTs with the decrease of the working pressure, which is attributed to enhanced densification, better surface morphology of the In_2O_3 channel layers prepared at lower deposition pressure. The fabricated TFT with optimal device performance exhibited a field-effect mobility (μ_{FE}) of 31.6 $cm^2\,V^{-1}\,s^{-1}$, a drain current on/off ratio of $\sim 10^7$, a low off drain current of about 10^{-10} A and a threshold voltage of 7.8 V. Good device performance and low processing temperature make the In_2O_3-TFTs suitable for the potential applications in the transparent electronics.

© 2009 Elsevier Ltd. All rights reserved.

1. Introduction

Very recently the development of TFTs based on transparent oxide semiconductors (TOSs) such as zinc oxide (ZnO), tin dioxide (SnO_2), indium–zinc oxides (IZO), indium–gallium–zinc oxide (IGZO) [1–6] and other transparent oxides have attracted considerable attention from researchers. The main advantages of TOSs used as active channel layers are their high electron mobility and good transparency in the visible spectral region. These excellent features make TOSs a promising candidate for replacing amorphous and poly-silicon thin films that have been widely used as the channel layers in active matrix liquid crystal displays (AMLCDs). Furthermore, owing to low processing temperature of TOSs, TFTs based on TOSs also show potential applications in the transparent flexible electronics. ZnO, a well-known representative of TOSs, has been recognized as a suitable material for TFTs. In order to optimize device performance, ZnO-TFTs have been widely studied via various processing techniques such as substrate heating, post-rapid thermal annealing (RTA) treatment and so on [7–9]. In_2O_3 is also a typical TOS material with a direct wide band gap of about 3.6 eV. In particular, the bottom of the conduction band of In_2O_3 consists of single free electron-like band of In 5s states hybridized with highly dispersed O 2s states, while the valence band edge arises from the O 2p states hybridized with In 5d states. This unique band structure results in uniform distribution of the charges that reduces the scattering to a minimum [10], which makes the In_2O_3 thin films exhibit high intrinsic mobility. These merits make In_2O_3 a more promising candidate to be used in practical transistors. Wang et al. [11] have reported high-performance transparent inorganic–organic hybrid n-type TFTs. In_2O_3 thin films were grown by ion-assisted deposition. Dhananjay et al. [12,13] have prepared In_2O_3 thin films by reactive evaporation of indium in ambient oxygen. The effect of various annealing treatments on the conductivity of the films for TFTs has been investigated. Wang et al. [14,15] have reported on the fabrication of In_2O_3-TFTs by reactive ion beam assisted deposition and conducted an investigation of material properties as a function of primary deposition parameters such as ion flux and deposition rate. Regarding all these cases, there are few investigations of device performance as a function of working pressure. In fact, it is well known that working pressure, as one of the main deposition parameters, has crucial effect on device performance. In this paper, we report on the fabrication and characterization of In_2O_3-TFTs. In_2O_3 channel layers were deposited on thermally grown silicon dioxide (SiO_2)/n-type silicon (Si) at room temperature (RT) by radio-frequency (RF) magnetron sputtering. Herein, the emphasis of this work is to study the effect of deposition pressure of In_2O_3 channel layers on the performance of In_2O_3-TFTs.

* Corresponding authors. Tel.: +86 574 86685161; fax: +86 574 86685163.
E-mail addresses: h_cao@nimte.ac.cn (H.T. Cao), Wanqing7686@hotmail.com (Q. Wan).

0038-1101/$ - see front matter © 2009 Elsevier Ltd. All rights reserved.
doi:10.1016/j.sse.2009.12.025

Author's personal copy

2. Experimental details

A typical bottom gate structure was used for the fabrication of In_2O_3-based TFTs. N-type Si(111) coated with a thermally grown 300 nm thick SiO_2 layer (capacitance per unit area C_i = 10 nF/cm^2) was selected as substrate. Si (ρ < 0.01 Ω cm) and SiO_2 acted as gate and gate dielectric layer, respectively. Indium was welded to n-type Si substrate as gate electrode by removing some part of SiO_2 layer. The contact between n-type Si and In electrode pad was confirmed to be ohmic contact. The In_2O_3 active layers were deposited on SiO_2/n-type Si substrates by a RF magnetron sputtering (ULVAC JSP-8000) using a commercially available 2 in. undoped In_2O_3 target (4 N) at RT. Before depositing the films, the substrates were ultrasonically cleaned with acetone, ethanol and deionized water for 30 min in each solution. Sequentially, the In_2O_3 target was pre-sputtered with a RF power of 100 W for 20 min in order to clean the target surface. Prior to deposition, the chamber was evacuated to $\sim 10^{-4}$ Pa. In this work, four samples were prepared, marked as A, B, C, and D. A, B and C samples were deposited for 50 min with a RF power of 100 W at the same Ar/O_2 flow rate ratio (3/1) but with various total gas-flow rate of 14 sccm, 10 sccm, and 6 sccm (corresponding to the total deposition pressure of 0.65, 0.45, 0.25 Pa), respectively. The D sample was deposited for 35 min at the same deposition condition as C. Some main deposition parameters are summarized in Table 1.

After deposition of the In_2O_3 channel, Ti/Au (50/100 nm) contacts as source and drain electrodes were subsequently deposited on the In_2O_3 channel layer through the shadow mask by electron beam evaporation (ULVAC MUE-ECO-EB). The channel width and length of In_2O_3-TFTs were 400 μm and 80 μm (W/L = 5), respectively. Finally, TFTs were treated by rapid thermal annealing (RTA) (RTP-500 V) at 300 °C for 1 min in air. The thickness and refractive index (n) of In_2O_3 thin films were analyzed by a spectroscopic ellipsometer (SE) (J.A.Woollam Co., Inc., M-2000DI) with a spectrum response range of 190–1700 nm. The crystallization property of In_2O_3 thin-film was evaluated by X-ray diffraction (XRD) measurement using D8 Advance spectrometer of Bruker AXS with Cu K_α (λ = 1.5418 Å) radiation in θ–2θ scan mode. The surface morphology and roughness of In_2O_3 films were observed via a scanning probe microscopy (SPM) (Veeco Dimention 3100). The electrical properties of In_2O_3-TFTs were measured using a semiconductor parameter analyzer (Keithley 4200) and the electrical contact to the DUT (Device Under Test) was connected through tungsten probes using a PM5 (SÜSS) micro-probe station. Hall-effect measurements were performed at room temperature using the Van der Pauw method (Ecopia hall-effect measurement system HMS-3000).

3. Results and discussion

3.1. Structural characteristic of In_2O_3 film

The crystallization properties of a typical sample were analyzed by the XRD technique, as shown in Fig. 1. (The other samples exhibited the same trend.)

Table 1
Some main deposition parameters of In_2O_3 channel layers.

Sample no.	Base pressure (Pa)	Ar:O_2	Deposition pressure (Pa)	Deposition time (min)	Thickness (nm)
A	2.0×10^{-4}	3:1	0.65	50	57
B	1.0×10^{-4}	3:1	0.45	50	68
C	1.2×10^{-4}	3:1	0.25	50	85
D	1.8×10^{-4}	3:1	0.25	35	54

It can be clearly seen that the as-deposited In_2O_3 thin-film shows amorphous feature, while the post-RTA-treated In_2O_3 thin film is polycrystalline without obvious preferred orientation. The diffraction patterns are in a good agreement with the cubic bixbyite structure of In_2O_3 film, which exhibit obvious peaks located at 30.78°, 35.70°, 51.27°, and 61.01°, corresponding to the (2 2 2), (4 0 0), (4 4 0) and (6 2 2) planes of In_2O_3 (standard PDF card No. 06–0416) [10], respectively. However, in comparison with the standard value, there is a slight shift to higher diffraction angle for the peak position, revealing the presence of stress in the post-RTA-treated In_2O_3 film.

3.2. Surface morphology of In_2O_3 film

The surface morphologies of as-deposited and post-RTA-treated In_2O_3 films deposited at different deposition pressure were examined via the SPM. SPM images of all samples were collected over a scanning area of 1 μm × 1 μm. Root-Mean-Square (RMS) roughness of all In_2O_3 films is presented in Table 2.

It is evident that RMS roughness decreases with the reduction of deposition pressure. Moreover, there is an increase in the RMS roughness of all post-RTA-treated films compared with as-deposited ones. The In_2O_3 thin films deposited at low deposition pressure exhibit very good surface morphology, as shown in Fig. 2.

The surface roughness of post-RTA-treated D-sample with optimal device performance and post-RTA-treated A-sample with poor device performance are 0.44 nm, 1.67 nm, respectively, which would be explained further in the subsequent section.

3.3. Thickness and refractive index characterization of In_2O_3 film

The thickness and refractive index of In_2O_3 thin films were obtained by fitting the ellipsometry spectra ranging from 190 to 1700 nm. Fig. 3 depicts the spectra of refractive index of the In_2O_3 films as a function of wavelength λ. The physics and dispersion model for the SE analysis are shown in the insets to Fig. 3.

It can be seen from the spectra that D-sample exhibits almost the same refractive index as C-sample, despite their different film thickness. It reveals that the refractive index is mainly affected by deposition pressure, rather than thin-film thickness. The refractive index at 500 nm is shown in Table 2. It is clear that the refractive index increases as deposition pressure decreases. The packing density was calculated using the following expression [16]:

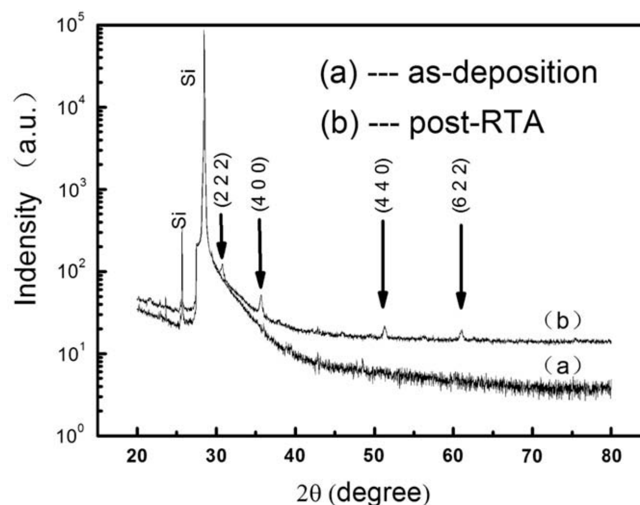

Fig. 1. The XRD pattern of D-sample (a) as-deposited and (b) post-RTA-treated.

Author's personal copy

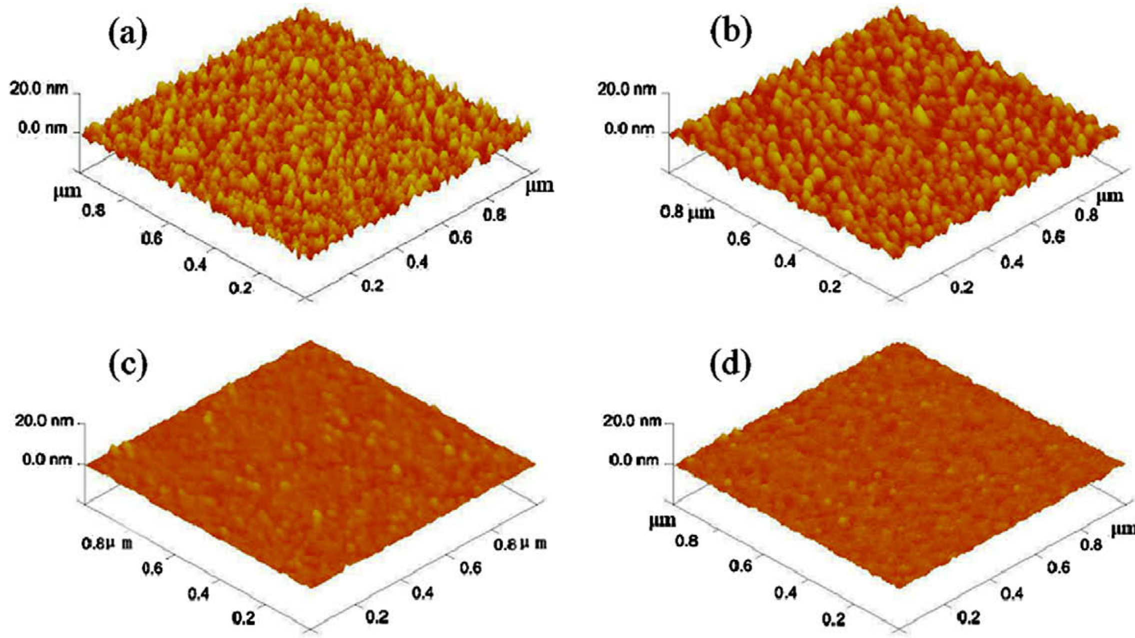

Fig. 2. SPM images of In_2O_3 films: (a) as-deposited A-sample (b) post-RTA-treated A-sample (c) as-deposited D-sample (d) post-RTA-treated D-sample with a scanning area of 1 µm × 1 µm.

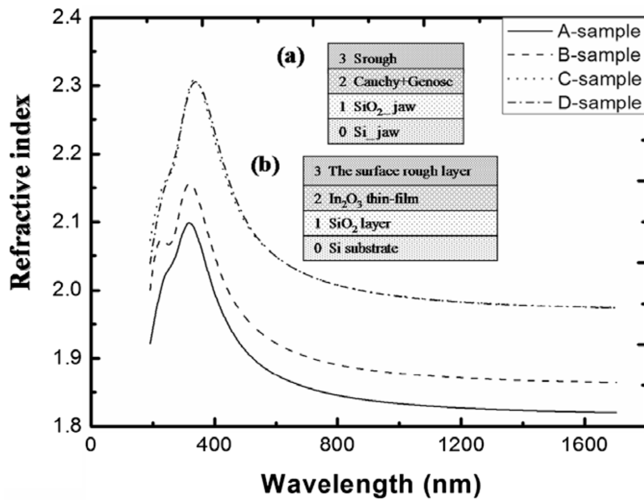

Fig. 3. The spectra of refractive index as a function of wavelength λ and the insets: (a) dispersion model (b) physics model for SE date analysis.

$$n_f^2 = \frac{(1-p)n_v^4 + (1+p)n_v^2 n_s^2}{(1+p)n_v^2 + (1-p)n_s^2}, \quad (1)$$

where n_f is the refractive index of the film at a specific wavelength, here λ = 500 nm, n_v the index of the voids (n_v = 1 for air), n_s the bulk value of refractive index and p the packing density. The calculated values of p are also presented in Table 2. It is speculated that the high packing density of the In_2O_3 film deposited at low deposition pressure would correlate well with the device performance, which would be explained in detail later on.

3.4. Electrical characterization of In_2O_3-based TFTs

The output characteristics (I_D–V_{DS}) and transfer characteristics ($\log_{10} I_{Dsat}$–V_{GS} and $\sqrt{I_{Dsat}}$–V_{GS}) of A sample and D sample are illustrated in Fig. 4. The electrical properties of all devices are calculated and summarized in Table 2.

Field-effect mobility (μ_{FE}) and subthreshold voltage swing (S) are two important performance parameters for TFTs applications. The μ_{FE} of In_2O_3-TFTs operating in the saturation region was extracted by taking the slopes of $\sqrt{I_{Dsat}}$–V_{GS} curves in Fig. 4, using the following equation:

$$I_D = \frac{WC_i\mu_{FE}}{2L}(V_{GS} - V_T)^2, \quad (2)$$

where C_i is the capacitance per unit area of the gate dielectric, V_T the threshold voltage obtained from the x-axis intercepts of $\sqrt{I_{Dsat}}$–V_{GS} plot, μ_{FE} the field-effect mobility, W and L are the channel width and length and V_{GS} is the gate-source voltage. The μ_{FE} was extracted from the unpatterned In_2O_3-TFTs without considering the fringing electric field effect [17]. The S values of In_2O_3-TFTs were extracted from the subthreshold region in the $\log_{10} I_{Dsat}$—V_{GS} plot, which is the voltage required to increase the drain current by a factor of 10:

$$S = \frac{dV_{GS}}{d\log(I_{DS})}. \quad (3)$$

As mentioned in the previous section, the post-RTA-treated In_2O_3 thin film is polycrystalline. Amorphous channel layer is generally superior to polycrystalline for practical application, however, there are higher density of point defects within the as-deposited films compared with post-RTA-treated ones and those point defects may act as deep-level traps, as reported in ZnO films [18,19], which would significantly affect the device performance. In our experiment the as-deposited and RTA-treated device performance was compared. It was found the post-RTA-treated In_2O_3-TFT exhibited obviously good performance compared with as-deposited In_2O_3-TFTs. So, all our TFTs employed a post-rapid thermal annealing treatment in this work.

It can be seen from Table 2 that the In_2O_3-TFTs deposited at lower deposition pressure exhibit obvious higher μ_{FE} values than those prepared at higher deposition pressure. Especially, the S value is 50.0, 27.0, 8.0 and 5.7 V/decade for A, B, C, and D sample, respectively, revealing significant improvement in the S parameter

Author's personal copy

Table 2
Refractive index, packing density, roughness and some main performance parameters for all samples prepared at different deposition pressure.

Sample no.	Refractive index (at 500 nm)	Packing density	As-deposition SPM RMS roughness (nm)	Post-RTA SPM RMS roughness (nm)	μ_{FE} ($cm^2\ V^{-1}\ s^{-1}$)	S (V/decade)	$I_{on/off}$ ratio	V_{th} (V)	I_{off} (nA)
A	1.91	0.93	1.35	1.67	0.02	50	2.1×10^2	−10	7.5
B	1.96	0.95	1.37	1.46	0.01	27	2.0×10^2	−37	4.1
C	2.10	1.02	0.93	0.99	34.8	8.0	3.7×10^5	−3.2	6.7
D	2.10	1.02	0.43	0.44	31.6	5.7	1.0×10^7	7.8	0.1

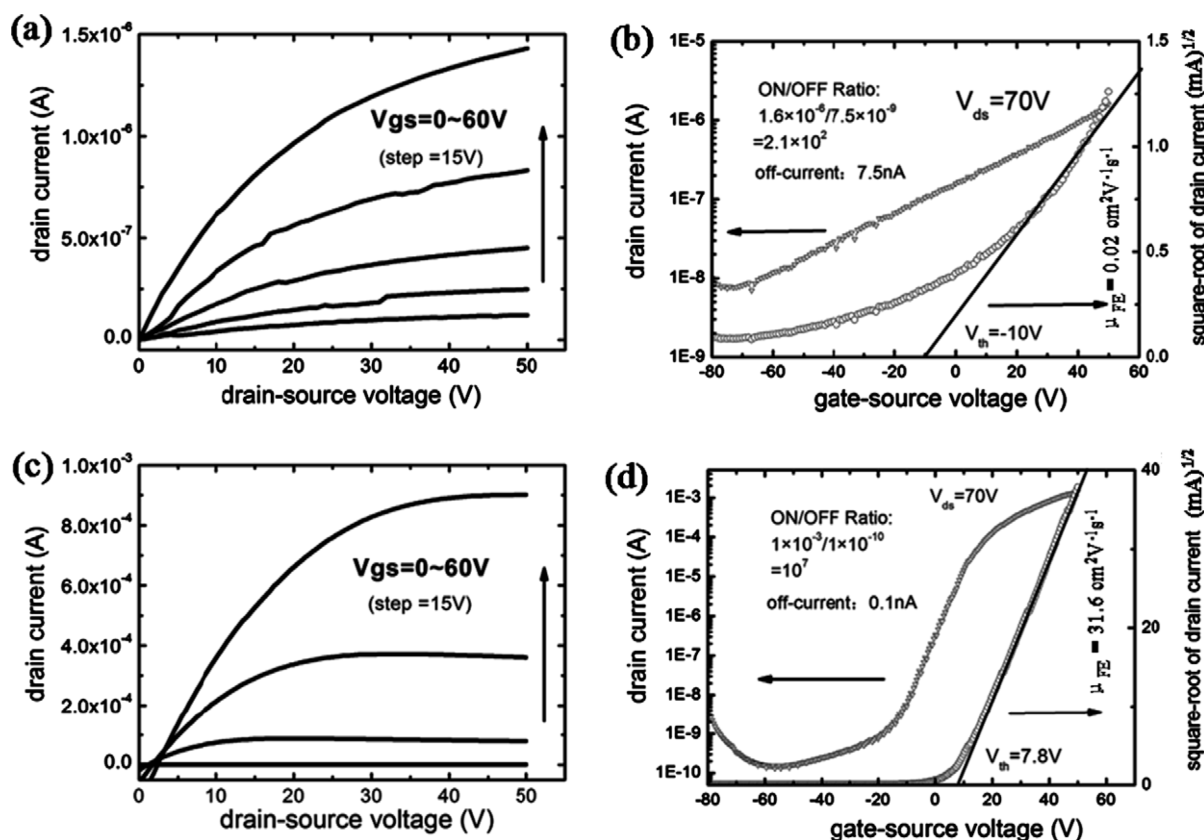

Fig. 4. (a) The output characteristics (I_D–V_{DS}) and (b) transfer characteristics ($\log_{10} I_{Dsat} \sim V_{GS}$ and $\sqrt{I_{DS}} \sim V_{GS}$) of A-sample; (c) the output characteristics (I_D–V_{DS}) and (d) transfer characteristics ($\log_{10} I_{Dsat} \sim V_{GS}$ and $\sqrt{I_{DS}} \sim V_{GS}$) of D-sample.

with the decrease of the deposition pressure. Why the In_2O_3-TFTs fabricated at lower deposition pressure exhibit better device performance? On one hand, the surface morphology has an important effect on the device performance, i.e., smooth surface morphology leads to a good interface between the source/drain electrodes and the In_2O_3 channel layers. Good interface ensures a reduced role of surface and interface states on carrier transport across the drain and source [13], resulting in an increased field-effect mobility. The surface morphology of In_2O_3 channel layers has been greatly improved with the reduction of deposition pressure, as shown in Fig. 2, resultantly presenting better device performance. On the other hand, it is generally believed that the μ_{FE} is greatly governed by the density of the tailing state near the conduction band (shallow trap), while the S is determined by the deep-level trap density. And the total trap (shallow trap and deep-level trap) density of the channel layer is well correlated with its densification [20]. In this study, it was found that the In_2O_3 channel layers deposited at lower deposition pressure exhibited higher refractive index and packing density, indicating an increase of densification and a corresponding decrease of total trap density in the bandgap of the In_2O_3 channel layer, which could further explain why TFTs prepared at lower deposition pressure exhibited better performance.

The effect of channel layer densification and surface morphology on the device performance can be confirmed by electrical properties of the indium oxide itself obtained through hall-effect measurement. The carrier concentration, resistivity and μ_{Hall} of sample A is $8.6 \times 10^{19}\ cm^{-3}$, $1.1 \times 10^{-1}\ \Omega\ cm$, $0.7\ cm^2\ V^{-1}\ s^{-1}$, and those of sample D is $1.9 \times 10^{18}\ cm^{-3}$, $1.8 \times 10^{-1}\ \Omega\ cm$, $18.2\ cm^2\ V^{-1}\ s^{-1}$, respectively. Although all TFTs were fabricated in the same Ar/O_2 flow ratio, sample A was prepared in higher total working pressure compared with sample D. In general, higher working pressure increases the scattering of the sputtered species, resulting in a decrease in mean free path of the incident atoms, which would lead to the less densification and poorer surface morphology of In_2O_3 channel layer as confirmed by the SE and SPM results. In addition, higher deposition pressure will induce a relatively larger number of intrinsic donor defects in the unintentional doped channel layer, which would cause an increase in the carrier concentration. Therefore, sample A presents a higher electron concentration compared with sample D. However, the large electron concentration will make it difficult for the TFT to operate

Author's personal copy

in saturation region and it is well consistent with no strong saturation in the output characteristics (I_D–V_{DS}) of sample A, as shown in Fig. 4. Moreover, a large number of intrinsic donor defects will act as the electron scattering centers, giving rise to the increase of S and decrease of both μ_{Hall} and μ_{FE}. From the above mentioned, it is concluded that the surface morphology along with the densification of the channel layer could account for the variation of device performance.

4. Conclusions

We have performed the fabrication and characterization of bottom-gate-type In_2O_3-based TFTs. The In_2O_3 channel layers were deposited on the thermally grown SiO_2/n-type Si substrates by RF magnetron sputtering at different deposition pressure. The XRD pattern reveals that the post-RTA-treated In_2O_3 film is polycrystalline without obvious preferred orientation. The performance of TFTs can be improved by decreasing the deposition pressure of channel layers, since low deposition pressure results in low surface roughness, high densification and enhanced electrical property of In_2O_3 channel layers. The fabricated TFT with optimal electrical performance exhibited a field-effect mobility (μ_{FE}) of 31.6 $cm^2\,V^{-1}\,s^{-1}$, a drain current on/off ratio of $\sim10^7$, a low off-current of about 10^{-10} A and a threshold voltage of 7.8 V.

Acknowledgments

The authors are grateful for the financial supports of the key project of The Natural Science Foundation of Zhejiang province, China (Grant No. 0804201051), Special Foundation of President of the Chinese Academy of Sciences (Grand No. 080421WA01).

References

[1] Wager JF. Transparent electronics. Science 2003;300:1245–6.
[2] Hoffman RL, Norris BJ, Wager JF. ZnO-based transparent thin-film transistors. Appl Phys Lett 2003;82:733–5.
[3] Presley RE, Munsee CL, Park CH, et al. Tin oxide transparent thin-film transistors. J Phys D: Appl Phys 2004;37:2810–3.
[4] Dehuff NL, Kettenring ES, Hong D, et al. Transparent thin-film transistors with zinc indium oxide channel layer. J Appl Phys 2005;97:064505.
[5] Nomura K, Ohta H, Takagi A, et al. Room-temperature fabrication of transparent flexible thin-film transistors using amorphous oxide semiconductors. Nature 2004;432:488–92.
[6] Yabuta H, Sano M, Abe K, et al. High-mobility thin-film transistor with amorphous InGaZnO4 channel fabricated by room temperature RF-magnetron sputtering. Appl Phys Lett 2006;89:112123-3.
[7] Masuda S, Kitamura K, Okumura Y, et al. Transparent thin film transistors using ZnO as an active channel layer and their electrical properties. J Appl Phys 2003;93:1624–30.
[8] Carcia PF, McLean RS, Reilly MH, et al. Transparent ZnO thin-film transistor fabricated by RF magnetron sputtering. Appl Phys Lett 2003;82:1117–9.
[9] Hossain FM, Nishii J, Takagi S, et al. Modeling of grain boundary barrier modulation in ZnO invisible thin film transistors. Physica E 2004;21:911–5.
[10] Raj AME, Lalithambika KC, Vidhya VS, et al. Growth mechanism and optoelectronic properties of nanocrystalline In2O3 films prepared by chemical spray pyrolysis of metal-organic precursor. Phys B: Condens Matter 2008;403:544–54.
[11] Wang L, Yoon MH, Lu G, et al. High-performance transparent inorganic–organic hybrid thin-film n-type transistors. Nature Mater 2006;5:893–900.
[12] Dhananjay, Chu CW. Realization of In2O3 thin film transistors through reactive evaporation process. Appl Phys Lett 2007;91:132111.
[13] Dhananjay, Cheng SS, Yang CY, et al. Dependence of channel thickness on the performance of In2O3 thin film transistors. J Phys D: Appl Phys 2008;41:092006.
[14] Wang K, Vygranenko Y, Chaji R, et al. Indium oxides by reactive ion beam assisted evaporation: from material study to device application. J Vac Sci Technol B 2009;27:612–7.
[15] Wang K, Vygranenko Y, Chaji R, et al. Stability of indium-oxide thin-film transistors by reactive ion beam assisted deposition. Thin Solid Films 2009;517:6341–4.
[16] Harris M, Macleod HA, Ogura S. Relationship between optical inhomogeneity and film structure. Thin Solid Films 1979;57:173–8.
[17] Okamura K, Nikolova D, Mechau N, et al. Appropriate choice of channel ratio in thin-film transistors for the exact determination of field-effect mobility. Appl Phys Lett 2009;94:183503-3.
[18] Lee JY, Choi YS, Choi WH, et al. Characterization of films and interfaces in n-ZnO/p-Si photodiodes. Thin Solid Films 2002;420:112–6.
[19] Zeng JN, Low JK, Ren ZM, et al. Effect of deposition conditions on optical and electrical properties of ZnO films prepared by pulsed laser deposition. Appl Surf Sci 2002;197:362–7.
[20] Jeong JH, Yang HW, Park JS, et al. Origin of subthreshold swing improvement in amorphous indium gallium zinc oxide transistors. Electrochem Solid State Lett 2008;11:157–9.